CHICKEN SWARM OPTIMIZED DEEP LEARNING NEURAL NETWORK CLASSIFIER FOR CYCLONE PREDICTION

Abstract

Predicting wind speed with high accuracy and reliability has become difficult for weather forecasters. Over the years, a number of forecasting methodologies have been introduced for precise forecasting of wind speed and combating the ambiguity of variation. To deal with this, we created a Convolution Neural Network (CNN)-based deep learning (DL) tropical cyclone (TC) intensity forecasting system. This research proposes an adaptive K-means image segmentation method that produces accurate results for segmentation with straightforward operation and does not require interactive K value input. Applying the gray level co-occurrence matrix (GLCM), characteristics are retrieved from the segmented images. An algorithm known as chicken swarm optimization (CSO) has been proposed and it has a high operational efficiency and quick convergence speed. The combination of DL and parameter optimizer employed by the described CSO-DL model is used to predict the cyclone. The experimental findings shows that the CNN classifiers achieves the greatest testing and training accuracy of 94.7% and 95.2% respectively. The development of this model can serve as a helpful benchmark for studies on cyclone prediction.

Keywords: Deep learning, CNN, Chicken Swarm Optimization, GLCM, Cyclone Prediction.

Authors

S. Raji
Lecturer
Department of Electronics and Communication Engineering
NSS Polytechnic College
Pandalam, Kerala, India.
srajisarathy56@gmail.com

A. T. R. Krishna Priya
PG Scholar
Department of Computer Science and Engineering
Rohini College of Engineering and Technology
Kanyakumari, Tamilnadu, India.
priya.gita6@gmail.com

R. Anuja
Assistant Professor
Faculty of Computer Science and Engineering
Rohini College of Engineering and Technology
Kanyakumari, Tamilnadu, India.
anujaryanalwin@gmail.com

D. Madhivadhani
Assistant Professor
Faculty of Electronics and Communication Engineering, Kings Engineering College
Chennai, India.
vadhaniece@gmail.com

I. INTRODUCTION

The tropics and subtropics of the world are significantly threatened socioeconomically by TCs. Effective TC route and intensity forecast can reduce TC losses and fatalities by providing actionable knowledge on TC threats. This has significant social advantages. While TC track prediction has taken tremendous strides over the past several decades, TC strength prediction has only slightly advanced [1, 2]. Powerful TCs have the potential to intensify into typhoons, which are unexpected natural disasters that cause yearly losses in human lives and property. The forecast of the TC's path is extremely difficult because of all these complicated issues. Thus, it is crucial to research and implement novel TC track forecasting methodologies considering the effect of TCs on society as well as the intricacy associated in their forecast. The basic foundations of conventional track forecasting methods are a mathematical approach and statistics equations. Despite the fact that these techniques have become increasingly common in tandem with the advancement of technological devices and tracking techniques, they remain to be hampered by significant complexity and comparatively poor forecasting precision [3-5]. Furthermore, these conventional approaches are constrained by their inherent limitations, which prevent them from analyzing included data features and force them to depend excessively on rules that are summed up by past information without taking into account the intricate relationships between meteorological factors and TC monitors on both attribute and spatial measurements. DL methods are now effectively used in identifying objects, processing natural languages, and processing images [6, 7]. They have demonstrated significant benefits in handling big quantities of complicated time-series information in two different ways. Initially using a CNN, for example, DL algorithms can better enhance their generalization abilities by extracting implicit characteristics from a dataset that span many variables. Thus, a DL methodology is a suitable strategy for our track forecasting investigation.

The substance of the photos will be impacted by the cyclone images' common traits, such as unpredictable sound, low contrast, inhomogeneity, weak borders, and unconnected portions. Pre-processing procedures helped to solve this issue. Preprocessing is a crucial part of image processing since it improves the image clarity for extraction of features and classification. The preprocessing procedures deal with noise reduction, image improvement, and removal of certain marks. For automated and semiautomatic picture segmentation, there were numerous methods available in the image segmentation phases. It is quite challenging to eliminate the noise and unique markings that are present in images because of the poor image contrary, uniformity weak limits, and noise [8, 9]. The technique of splitting a picture into a number of meaningful, separate sections that have the same properties is known as image segmentation. The precision of picture segmentation, an essential technology in image processing, impacts the success of the subsequent activities. The present segmentation method has had different degrees of success given its level of complexity and challenge, but further study in this area still confronts many obstacles. The clustering research method splits data sets into multiple categories in accordance with a predetermined standard; as a result, it finds extensive use in the segmentation of images. Our methodology, which relies on the initial technique, enhances both the design of the program and its precision of picture segmentation [10, 11]. In the meantime, this work suggests a novel approach for calculating K in the K-means clustering algorithm. The image segmentation technique presents in our paper has found widespread use and produced effective results for cyclone picture. In this research, the GLCM is employed to extract texture data.

Bio-inspired meta-heuristic algorithms have effectively handled numerous optimisation challenges [12]. They take advantage of the optimization issues' sensitivity for ambiguity and inaccuracy to produce workable solutions at cheap computational cost. As a result, meta-heuristic algorithms to deal with optimization uses, such as PSO [13], ACO [14], and BAT [15], have gained a lot of research attention. Each of these algorithms derive swarm intelligence from the natural principles governing biological structures. The process of using what we can learn from nature to improve algorithms is currently ongoing.

In this research, a CNN-based DL TC intensity forecasting system is proposed where distortion in the image pre-processing is reduced using a median filter, and the image is further segmented using K-means to accurately estimate the TC and a novel bio-inspired optimization approach called CSO is presented to train CNN.

II. RELATED WORKS

Jie Lian et al [2020] [16] have developed a unique geographical location-based DL model to forecast tropical storm tracks utilizing a variety of meteorological variables. A CNN, a GRU layers and a multidimensional feature selection layer make up this model. Our suggested model is capable of handling data from time series efficiently and enhance generalizability. In the future, we are going to contrast our suggested approach with more contemporary numerical and statistical techniques and enhance the model through taking into account numerous TC and TC’s intensities.

Snehlata Shakya *et al* [2020] [17] have made a study for improving the spatial resolution and feature diversifications in an existing dataset, the interpolation and data enhancement approaches are used. CNN are employed to identify photos as either storm or nonstorm using the artificially enhanced data as a training set. It is anticipated that categorization performance will have an impact on cyclone eye location performance. Because of the curve of the planet's surface, flat photos are ineffective and will need to be added individually in the future, if they become available.

Pingping Wang et al [2020] [18] have discussed OSIP, a two-step technique based on DL network identification of objects and IP, is developed to locate the TC centre by analysing TC properties such as architecture and shape in satellite IR images. OSIP is highly effective and universal since it does not require the ergodic approach for estimation of parameters. Future research can create a more ideal framework using reliable central data to successfully fulfill the challenging task of predicting the TC intensity in real time.

Le Liu et al [2019] [19] have demonstrated a group of pathways characterizing a volatile process may be condensed into a representative set, which can then be utilized to create a representation that subtly conveys the ambiguity through its spatial distribution. If it is not essential to maintain the initial recordings but acceptable to create a new set that maintains the spatial distribution of the original set, our method can be used. Our technique divides the set into roughly equal-sized subsets by iteratively finding median pathways, which creates a set of sample tracks. If the technique were to be employed in a live event, more work would be required in order to enhance it.

Hui Li *et al* [2020] [20] have developed a hierarchical generative adversarial network (HGAN) to generate future imagery from satellites of typhoon clouds, providing a visual way for forecasting them. A local discriminator plus a global generator make up the HGAN. Its hierarchy structure and several subnetworks, which record all of the typhoon fluctuations and favour producing distinct future typhoon cloud images, are how it is built. In an HGAN, two networks constantly compete with one another, which can cause training to be unreliable and sluggish. Furthermore, HGANs frequently need a lot of training data for them to perform well.

III. PROPOSED SYSTEM

An original method for detecting and classification of cyclones is presented, one that makes use of the K-means segmentation method with selectively GLCM feature selection. The detailed structure of the suggested method is shown in Figure 1.

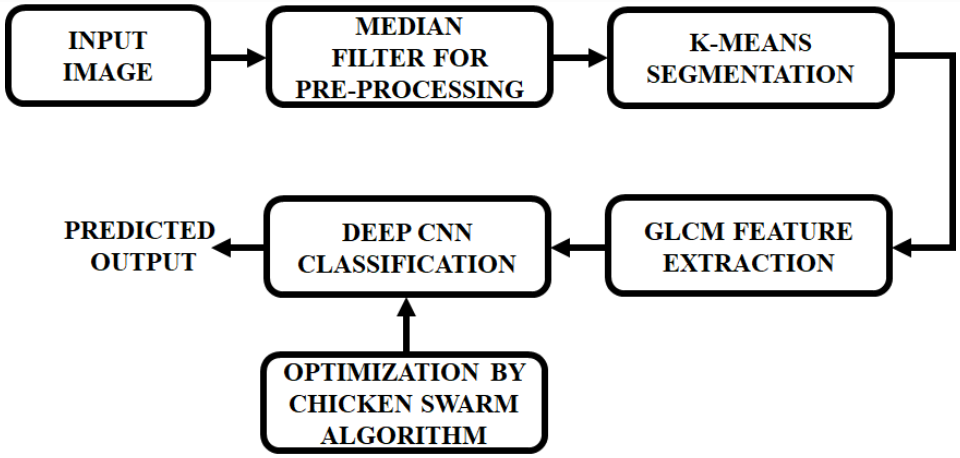

Figure 1: Proposed network

Figure 1 shows the suggested method for locating TC via analysing images. The system's input is an image of the cyclone. After using a median filter to reduce unwanted noise, the pre-processing of this shot improves its aesthetic appeal. We first increase the contrast of the input photo before using the k-means method to separate the images in order to detect the cyclone. The extraction of multiple properties, including colour, texture, and entropy-controlled most dominating qualities, is necessary for categorizing images. After the output of CNN is trained using a CSO method with a specific structure for the cyclone characteristic and the training variables, the result is forecasted using GLCM to compute the peculiar dependence of gray levels in an image.

1. **Image Preprocessing:** Pre-processing is largely used to improve image quality and set the stage for further processing by removing or reducing the irrelevant and unnecessary background features in mammography images. Pre-processing is thus required to improve quality. We pre-processed the photos before training the data. By removing the unnecessary and distracting features, this process improves the model's effectiveness. The preprocessing processes with a few modifications that worked best for the data we used.

The dataset's raw picture was trimmed to get rid of the header files and white edges. The photos were then subjected to image multiplication with a few further modifications. This step's goal was to eliminate extraneous details like grid lines, geographic boundaries, and landscape. In the traditional method of image binarization, pixels with intensities greater than a predetermined threshold are transformed to one, while those with lower intensities are changed to zero. The result of our program continued to be an image, but the pixels with intensity above a certain threshold kept their initial values, while the remaining pixels were changed to the minimum or zero. As a consequence, other elements were eliminated while just the vortex and surrounding cloud patches remained with their original pixel values. The threshold was chosen to be an appropriately optimized multiple (often 1.4) of the image's median pixel intensity. The produced image was then subjected to image erosion, the high frequency and noise elements are eliminated by filters.

Median filtering - A median filter is a linear Gaussian filter that is used to minimise noise from impulses in photographs. A nonlinear filter known as a median filter is used to minimise noise during preprocessing. Additionally, it is employed to keep an image's edges intact. The median value of nearby values is used to substitute each value in the filter. The neighbours of the filter frame the scene. This is going to be applied to the whole picture. Additionally, depending on how much of the original matrix is visible through the filter window, every component of the null matrix will modify the value it holds to the middle value in the initial matrix. Depending on the dimension of the filter window, the operation will be continued till any values in the null matrix change to the median value of the initial matrix.

A digital image with m rows and n columns in the two-dimensional sequence can be represented by

$$\{f(t,s); t = 1,2,\dots,m; s = 1,2,\dots,n\} \quad (1)$$

The two-dimensional array median filter's output is therefore

$$O(x,y) = \text{med}\{f(t,s)\}, (t,s) \in A(x,y) \quad (2)$$

2. **Segmentation By *K*-Means Algorithm:** K-means is one of the basic algorithms for clustering used in the partitioning approach. By grouping the K points in the space, the K-means algorithm's fundamental notion is to group the items that are nearest to each other. The measurements of each cluster's centroid are adjusted repeatedly until the best clustering outcomes are attained. A common example of a clustering technique based on the prototype function is the K-means algorithm. The target value of optimization is the distance between the data point and the prototype. The approach of discovering extreme parameters for functions is used to get the iterative adjustment procedures. The K-means algorithm uses Euclidean distance as a comparable metric to obtain the best classification for a cluster centre vector at the beginning of the process so that the index of evaluation is as small as possible. As a clustering criteria function, the error square sum requirement is employed. While the K-means method is effective, the quantity of K must be specified beforehand, and it is extremely hard to figure out the value of K. Frequently, the number of groups into which the provided data collection should be split is unknown beforehand.

This approach is highly efficient, but because it requires knowing how many clusters there are, K, it poses some challenges for automated calculations. The K values for the K-means segmentation method are determined using a combination of method for the most linked area and K-means. Extensive testing has revealed that K typically has a value between 2 and 10. To determine an accurate K value, we restore the image to just include the target item using the maximum connected domain algorithm, record the result, and then contrast it to the K value. The steps of the algorithm are listed below:

start K from 2 to 10

choose random K cluster centroids $\mu_1, \mu_2, \ldots, \mu_k \in R^n$

If $K \leq 10$, repeat{
For each pixel $x^{(l)}$

$e^{(l)}$=index (from 1 to K) of cluster centroid closest to $x^{(l)}$
For k=1 to K

μ_k: −mean of points assigned to cluster k
Compare the findings for the most related domains.
If right ,print results, break;
Else K=K+1;
}

This adaptive K-means method's pseudo code demonstrates how, when selecting the K value, it begins at 2 and gradually rises to 10. Our extensive set of research results show that cluster K is often chosen between 2 and 10. The K-means technique's success depends on choosing the right K value. We begin by choosing K = 2, which means that the segmentation of the image begins with two clusters. The total amount of segmentation results is ultimately determined using the greatest associated domain method. The K value has been chosen successfully if the final segmentation result's number of images equals it. If the K value is different, it will be raised until the two numbers mentioned above agree.

3. **Extraction Of Texture Teatures Using GLCM:** The particular dependence of the gray levels in an image is determined utilising the GLCM. The total amount of rows and columns and the total amount of gray levels in the image are identical in GLCM. Co-occurrence matrices can be built in four different spatial orientations: 0°, 45°, 90°, and 135°. The average of the previous matrices is used to generate another matrix. Let $\boldsymbol{P_{i,j}}$ represent the co-occurrence matrix and NxN represent the matrix's size. The frequency that a pixel with gray level i is spatially connected to a pixel having gray level j is represented by each element (i,j). Figure 2 shows the creation of GLCM from a grayscale image.

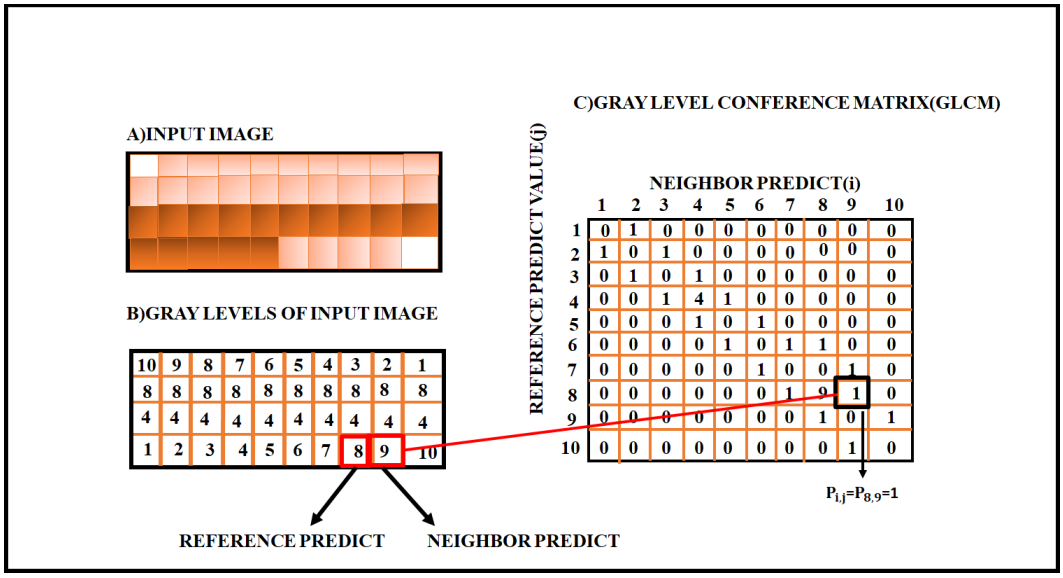

Figure 2: Construction of GLCM from an image

The example input image has 10 different shades of gray. GLCM depicts the relationship between neighbouring pixels (i) and (j) in a variety of orientations. The relationship between the pixels is determined in this instance horizontally and to the right (0°). Each of the items in GLCM (i, j) has a zero value at the beginning. Each element's value is modified based on how many pixels are present at once. Contrast, correlation, dissimilarity, energy, homogeneity, are texture features that can be determined using GLCM. Table 1 contains the formulas for calculating these attributes.

Table 1: Formulas to Calculate Texture Features from GLCM

SI.NO	GLCM Feature	Formula
1.	Contrast	$\sum_{i,j=0}^{N-1} P_{i,j}\,(i-j)^2$
2.	Dissimilarity	$\sum_{i,j=0}^{N-1} P_{i,j}\,(i-j)$
3.	Homogeneity	$\sum_{i,j=0}^{N-1} \frac{P_{i,j}}{1+(i-j)^2}$
4.	Energy	$\sum_{i,j=0}^{N-1} P_{i,j}^{2}$
5.	Correlation	$\sum_{i,j=0}^{N-1} P_{i,j}\,[\frac{(i-\mu_i)(j-\mu_j)}{\sqrt{(\sigma_i^2)(\sigma_j^2)}}$

4. **Deep Convolutional Neural Network:** Multiple layers of neurons make up a common deep CNN model and each layer extracts varying levels of non-linear information from the input, including low to high level features. The output of local convoluted filters in each layer is subjected to a nonlinear activation equation in order to produce nonlinearity in every layer.

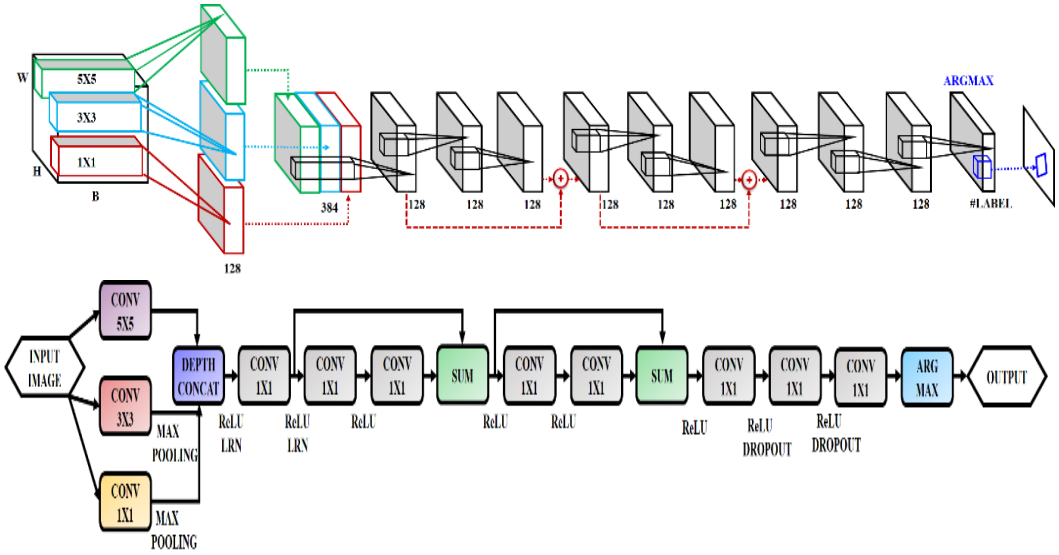

Figure 3: CNN Architecture

The connections between the input and output blobs of the convolutional layers are shown in the first row. Each convolutional layer's output blob includes an indication of how many filters are present. A system flowchart can be seen in the second row.

In order to lay the groundwork to understand the structure of the proposed network, we first outline the design of Alex Net, a popular deep CNN model, as depicted in Figure 3. Three fully linked layers and five convolutional layers make up Alex Net. Each layer that is fully linked has linear weights WF C that represent the connection between the input x and output y relationship.

$$y = W_{FC}.x, \tag{4}$$

Where the input and output vectors are represented by x and y. Local nonlinear features are extracted from the input via a convolutional layer with N local filters $W_{C.i}$, i = 1, 2,..., N, and are written as:

$$y = \{W_{C.i} * x\}_{i=1,2,\ldots,N}, \tag{5}$$

When there is a convolution, and. All $W_{C.i}$,i=1,2,...,N have carefully calculated filter sizes that are substantially smaller than the size of WF C. Several non-linear elements are utilized in equation (6), including dropout, softmax, the ReLU, and LRN. In order to extrapolate filter reactions, LRN restores each stimulation ai over localized activations of n adjacent filters centered on the location (p_x, p_y).

$$a_i^*(p_x, p_y) = a_i(p_x, p_y)/(k + \alpha \sum_{j=i-n/2}^{i+n/2}(a_j(p_x, p_y))^2)^\beta, \quad (6)$$

Where the hyper-parameters k, n are present. Max pooling, which is frequently employed for decreasing dimensionality in CNN, down samples the result of layers by substituting a portion of the output with the highest possible value. ReLU reduces values that are negative to zero and is utilized by the system to only learn parameters that have positive activations. Dropout, a function that accepts any value between 0 and 1, compels the output of each layer's individual nodes to be probability zero below a predetermined threshold. In this study, we made use of a 0.5 threshold. Dropout lessens excessive fitting concurrent multiple training data adaptations (also known as "complex coadaptations"). The logistic function, also known as the gradient-log-normalizer of the categorical probability distribution, is a generalization known as softmax.

$$P(y = j|x, \{f_k\}_{k=1,2,\ldots,K}) = \frac{e^{f_j(x)}}{\sum_{k=1}^{K} e^{f_k(x)}}, \quad (7)$$

When the input and output of the classification function f_j , for the j^{th} class are x and y, respectively. For probabilistic multiclass categorization, especially HSI classification, softmax is hence helpful.

5. **Chicken Swarm Optimization Algorithm:** The CSO approach is used to lower the Mean Square Error (MSE) by optimally modifying the CNN model's hyperparameters. The CSO method's high parallelism and flexibility make it favoured over other optimization strategies. The CSO imitates a chicken swarm's behavior and activity, and it is defined as follows: Each of the several groups that make up CSO has some chicks, hens, and a dominating rooster. In accordance with the fitness function, the amount of chicks, roosters, and hens is decided. The chicken that has the highest fitness rating is referred to as the rooster (group leader). The chicken with the lowest fitness value, though, is the chick. The majority of chickens are hens, and they are deliberately kept in that category.

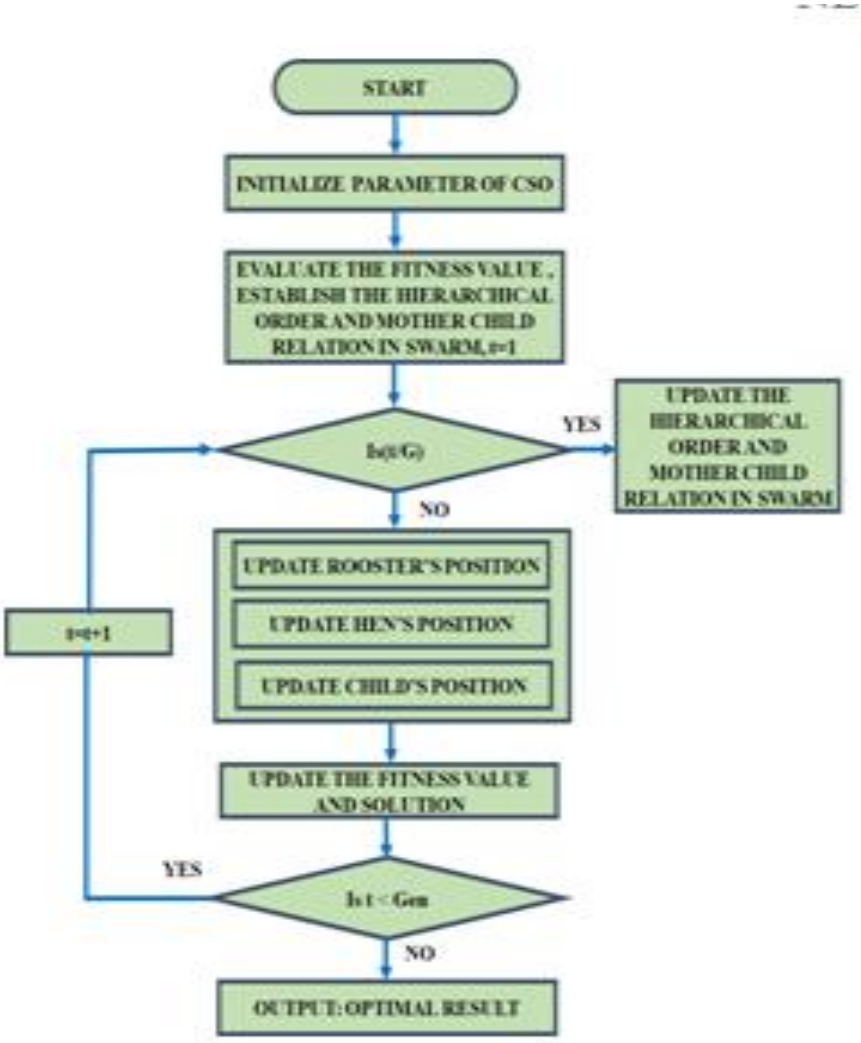

Figure 4: Flowchart of CSO

In the (G) time step, the group's mother-child and dominance linkages both remain the same and improve. To update the rooster's location, the equation for the chicken motion is provided below.

$$X_{ij}^{r+1} = X_{ij}^{t} * (1 + \text{randn}(0, \sigma^2)) \quad (8)$$

Where,

$$\sigma^2 = \begin{cases} 1 & \text{iff}_k \geq f_i \\ \exp\left(\frac{f_k - f_i}{|f_i + \varepsilon|}\right) & \text{otherwise} \end{cases} \quad (9)$$

Where $k \in [1, N_r], k \neq i$, and the total amount of roosters is N_r. In this example, $X_{i,j}$ stands for the position of rooster count i in the j^{th} dimension at the moment t during the t+1 iteration, randn $(0,\sigma^2)$ generates a random Gaussian integer with mean 0 and variance σ^2 , ε stands for a constant with the smallest value, and f_i stands for the fitness score of the corresponding rooster i: The hen modifying location is used in the subsequent equation (10).

$$X_{ij}^{r+1} = X_{ij}^{t} + S_1 \text{randn}\left(X_{r1,j}^{t} - X_{i,j}^{t}\right) + S_2 \text{randn}\left(X_{r2,j}^{t} - X_{i,j}^{t}\right) \quad (10)$$

In which S_1 is calculated in (11)

$$S_1 = \exp\left(\frac{f_i - f_{r1}}{|f_i| + \varepsilon}\right) \quad (11)$$

Then replace S_1 in equation (12)

$$S_1 = \exp\left(f_{r2} - f_i\right) \quad (12)$$

While $r1, r \in [1, \ldots, N], r1 \neq rr$ specifies the index of the rooster, $r2$ denotes the hen or rooster in the swarm, and randn is used to generate an arbitrary value with a uniform distribution. Finally, the following equation implements the chick updating position:

$$X_{ij}^{r+1} = X_{ij}^{t} + FL\left(X_{m,j}^{t}, X_{i,j}^{t}\right), FL \in [0,2] \quad (13)$$

Now $X_{m,j}^{t}$ shows the place of i^{th} chick mother

IV. RESULTS AND DISCUSSION

The TC Identification via Image Processing method suggested in this work is carried out utilizing the Python software platform. The results of simulation are produced by the median filter with image processing technique. Original TC pictures are represent in Figure 5.

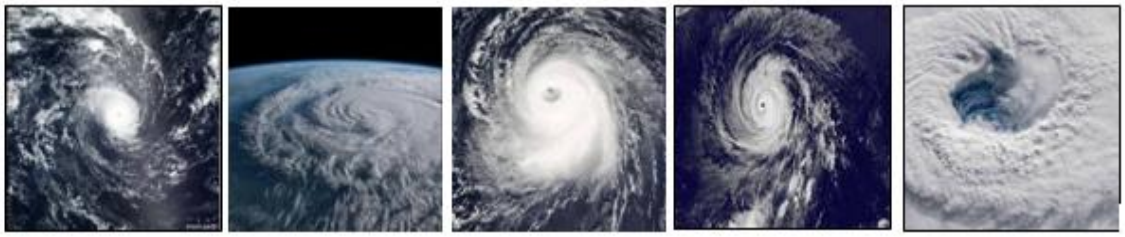

Figure 5: Original Image

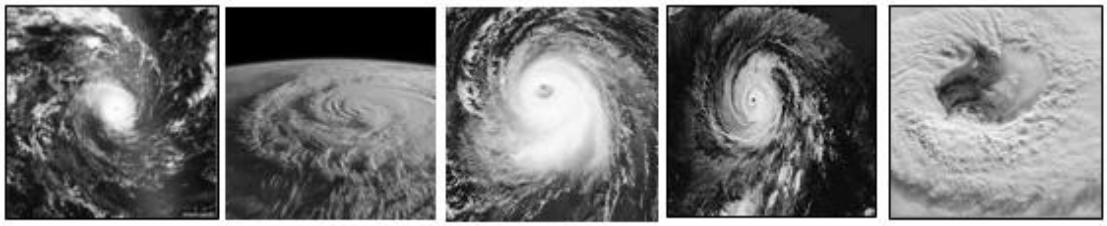

Figure 6: Gray Scale

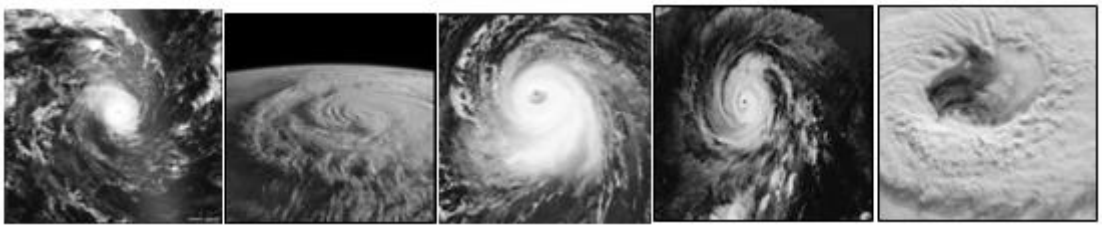

Figure 7: Median Filter

The median filter method has been used to filter an image. It is employed on the TC image to keep some elements while getting rid of others. Preprocessing is primarily used to enhance the appearance of TC images, but it can also enhance a number of other aspects of TC images, such as increasing their visual appeal, removing extra noise and unwelcome background elements, improving the interior of the region, and preserving its edges. Therefore, the proposed median filter enhances TC image quality while reducing noise.

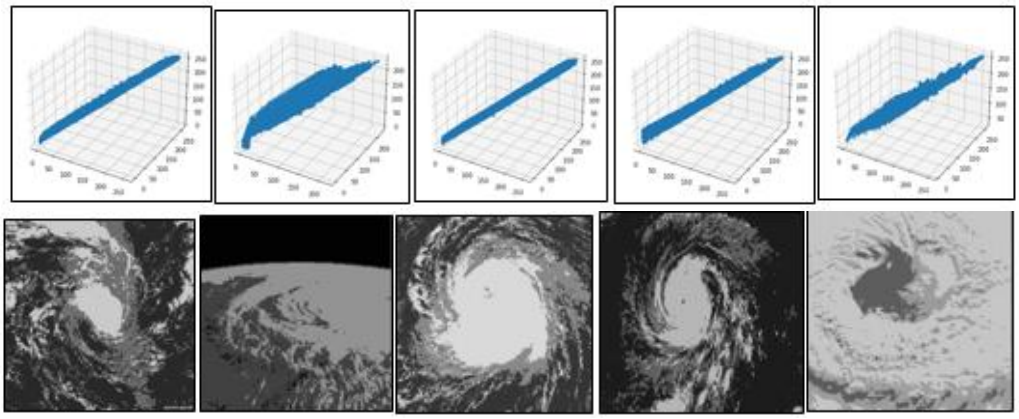

Figure 8: K-Means Segmentation

Here the images are divided into segments in order to make simpler to analyze, is required. It is intended to pinpoint various boundaries, including lines, circles, and curves. The segmentation of the image (retinal vessel segmentation) establishes whether a specific pixel represents a vessel or not. The K-Means Segmentation technique was used to create the segmented TC image in this case, and the results are displayed in the Figure above. It is tested against the conventionally known vascular network and displays unmistakably successful results.

Table 2: Feature Extraction

Images	**Extracted feature**				
	Homogeneity	**Correlation**	**Dissimilarity**	**Energy**	**Contrast**
Image.1	0.09624	0.89214	19.79704	0.01122	863.14482
Image.2	0.38106	0.97395	7.82335	0.19307	195.86033
Image.3	0.15318	0.91467	18.14730	0.01653	864.32641
Image.4	0.15662	0.89984	16.76999	0.03249	713.55068
Image.5	0.18422	0.95835	7.20654	0.02194	115.55706

The collection of data for the extraction of characteristics which includes homogeneity, energy, dissimilarity contrast, and correlation are shown in the aforementioned table. The results have been acquired using the GLCM technique on datasets. To pick appropriate features for the classifier's development is the main goal of feature selection. In this work, the CSO-based feature selection approach is used; it has the benefits of quicker training times, reduced overfitting, and avoidance of the dimensional problem while still producing the model.

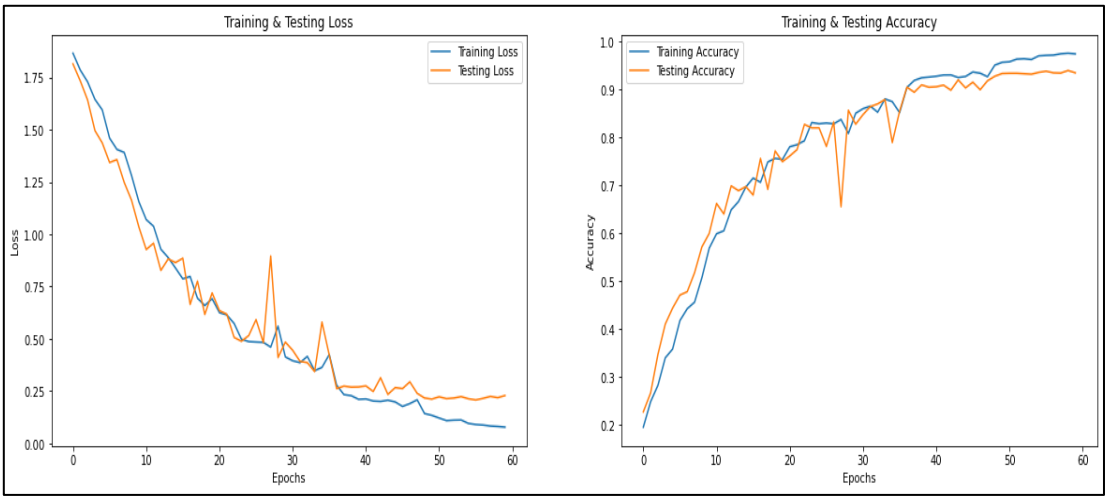

Figure 9: Accuracy & loss of CNN classifier

The accuracy and loss of the CNN classifier's testing and training periods are shown in Figure 9. The suggested CNN classifier has better accuracy loss with reduced testing & training loss, as shown by the graph. The suggested method successfully recognizes TC in colored photos as a consequence.

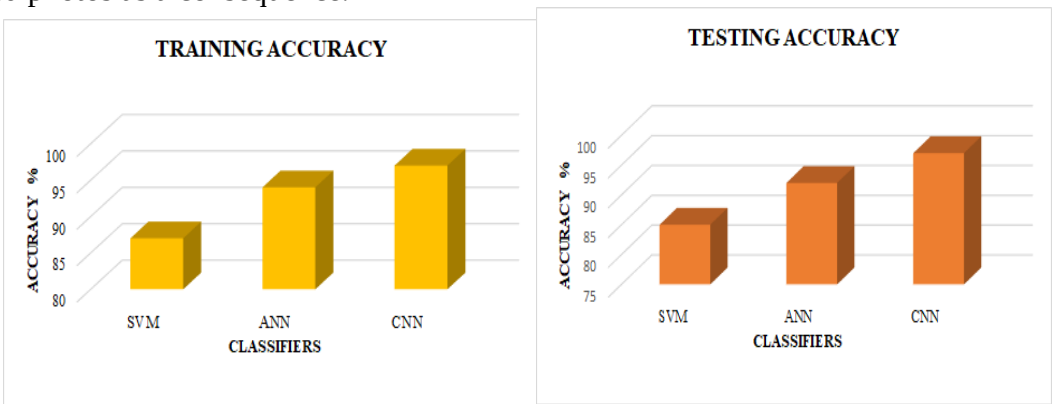

Figure 10: Comparison analysis of classifier accuracy

Figure 10 shows a comparison analysis of the training and testing accuracy of classifiers. It is clear from the findings that the suggested CNN classifier .

V. CONCLUSION

The lives of people and the environment have both been significantly impacted by TC. As massive volumes of meteorological and surveillance data continue to amass, traditional methodologies for forecasting TC tracks confront new hurdles in terms of forecasting efficacy and accuracy. Recent research has demonstrated that DL approaches are highly efficient and precise at predicting data in complex systems. From a large number of datasets, they may learn about both spatial and temporal characteristics. In this research,

utilizing historical data on TCs and a variety of meteorological variables, we suggested a unique DL model based on CNN models to forecast the TC's courses. K-means clustering technique is utilized for image segmentation, and GLCM is employed for feature extraction. The CSO algorithm is used, which lowers the error, to alter the CNN strategy hyperparameters in the best possible way. The hybrid DL and hyperparameter optimizer employed by the described CSO-DL model is used to calculate the cyclone. The experimental findings shows that the CSO-CNN model has the highest nonlinear fitting and generalization capabilities, the best precision and a low absolute average error value. CNN classifiers achieves the greatest testing and training accuracy of 94.7% and 95.2% respectively.

REFERENCES

[1] C. -J. Zhang, Q. Luo, L. -J. Dai, L. -M. Ma and X. -Q. Lu, "Intensity Estimation of Tropical Cyclones Using the Relevance Vector Machine From Infrared Satellite Image Data," in IEEE Journal of Selected Topics in Applied Earth Observations and Remote Sensing, vol. 12, no. 3, pp. 763-773, March 2019.

[2] Camargo, Suzana J., Joanne Camp, Russell L. Elsberry, Paul A. Gregory, Philip J. Klotzbach, Carl J. Schreck III, Adam H. Sobel et al. "Tropical cyclone prediction on sub seasonal time-scales." Tropical Cyclone Research, Vol.8, no. 3, pp: 150-165, 2019.

[3] Richman, Michael B., Lance M. Leslie, Hamish A. Ramsay, and Philip J. Klotzbach. "Reducing tropical cyclone prediction errors using machine learning approaches." Procedia computer science, Vol.114, pp: 314-323, 2017.

[4] Pan, Bin, Xia Xu, and Zhenwei Shi. "Tropical cyclone intensity prediction based on recurrent neural networks." Electronics Letters, Vol.55, no. 7, pp: 413-415, 2019.

[5] Leroux, Marie-Dominique, Kimberly Wood, Russell L. Elsberry, Esperanza O. Cayanan, Eric Hendricks, Matthew Kucas, Peter Otto, Robert Rogers, Buck Sampson, and Zifeng Yu. "Recent advances in research and forecasting of tropical cyclone track, intensity, and structure at landfall." Tropical Cyclone Research and Review, Vol.7, no. 2, pp: 85-105, 2018.

[6] Moses, Oliver, and Samuel Ramotonto. "Assessing forecasting models on prediction of the tropical cyclone Dineo and the associated rainfall over Botswana." Weather and climate extremes, Vol. 21, pp: 102-109, 2018.

[7] Heming, J. T. "Tropical cyclone tracking and verification techniques for Met Office numerical weather prediction models." Meteorological Applications, Vol.24, no. 1, pp: 1-8, 2017.

[8] Zhang, Chuang, Ming Wu, Jinyu Chen, Kaiyan Chen, Chi Zhang, Chao Xie, Bin Huang, and Zichen He. "Weather visibility prediction based on multimodal fusion." IEEE Access, Vol.7, pp: 74776-74786, 2019.

[9] Kumar, Shubham, Preet Lal, and Amit Kumar. "Turbulence of tropical cyclone 'Fani'in the Bay of Bengal and Indian subcontinent." Natural Hazards, Vol.103, no. 1, pp: 1613-1622, 2020.

[10] Alam, Md Morshedul, Zanbo Zhu, Berna Eren Tokgoz, Jing Zhang, and Seokyon Hwang. "Automatic assessment and prediction of the resilience of utility poles using unmanned aerial vehicles and computer vision techniques." International Journal of Disaster Risk Science, Vol. 11, pp: 119-132, 2020.

[11] Zhang, Changjiang, Lijie Dai, Leiming Ma, Jinfang Qian, and Bo Yang. "Objective estimation of tropical cyclone innercore surface wind structure using infrared satellite images." Journal of Applied Remote Sensing, Vol.11, no. 4, pp: 046030-046030, 2017.

[12] Singh, Prashant, Ivo Couckuyt, Khairy Elsayed, Dirk Deschrijver, and Tom Dhaene. "Multi-objective geometry optimization of a gas cyclone using triple-fidelity co-kriging surrogate models." Journal of Optimization Theory and Applications, Vol.175, pp: 172-193, 2017.

[13] S. Jin, X. Li, X. Yang, J. A. Zhang and D. Shen, "Identification of Tropical Cyclone Centers in SAR Imagery Based on Template Matching and Particle Swarm Optimization Algorithms," in IEEE Transactions on Geoscience and Remote Sensing, vol. 57, no. 1, pp. 598-608, Jan. 2019.

[14] X. -Y. Gao, J. -W. Li and C. -X. Zhang, "Similarity Calculation of 3D Model By Integrating Improved ACO Into HNN," in IEEE Access, vol. 8, pp. 155378-155388, 2020.

[15] A. M. Alhassan and W. M. N. W. Zainon, "BAT Algorithm With fuzzy C-Ordered Means (BAFCOM) Clustering Segmentation and Enhanced Capsule Networks (ECN) for Brain Cancer MRI Images Classification," in IEEE Access, vol. 8, pp. 201741-201751, 2020.

[16] J. Lian, P. Dong, Y. Zhang, J. Pan and K. Liu, "A Novel Data-Driven Tropical Cyclone Track Prediction Model Based on CNN and GRU With Multi-Dimensional Feature Selection," in IEEE Access, vol. 8, pp. 97114-97128, 2020.

[17] S. Shakya, S. Kumar and M. Goswami, "Deep Learning Algorithm for Satellite Imaging Based Cyclone Detection," in IEEE Journal of Selected Topics in Applied Earth Observations and Remote Sensing, vol. 13, pp. 827-839, 2020.

[18] P. Wang, P. Wang, C. Wang, Y. Yuan and D. Wang, "A Center Location Algorithm for Tropical Cyclone in Satellite Infrared Images," in IEEE Journal of Selected Topics in Applied Earth Observations and Remote Sensing, vol. 13, pp. 2161-2172, 2020.

[19] L. Liu, L. Padilla, S. H. Creem-Regehr and D. H. House, "Visualizing Uncertain Tropical Cyclone Predictions using Representative Samples from Ensembles of Forecast Tracks," in IEEE Transactions on Visualization and Computer Graphics, vol. 25, no. 1, pp. 882-891, Jan. 2019.

[20] H. Li, S. Gao, G. Liu, D. Guo, C. Grecos and P. Ren, "Visual Prediction of Typhoon Clouds With Hierarchical Generative Adversarial Networks," in IEEE Geoscience and Remote Sensing Letters, vol. 17, no. 9, pp. 1478-1482, Sept. 2020.

